

Nonsteroidal Anti-inflammatory Drugs Inhibit Vascular Smooth Muscle Cell Proliferation by Enabling the Ca^{2+} -dependent Inactivation of Calcium Release-activated Calcium/Orai Channels Normally Prevented by Mitochondria^{*S}

Received for publication, October 29, 2010, and in revised form, March 7, 2011. Published, JBC Papers in Press, March 14, 2011, DOI 10.1074/jbc.M110.198952

Eva Muñoz[‡], Ruth A. Valero[‡], Ariel Quintana^{§1}, Markus Hoth[§], Lucía Núñez[‡], and Carlos Villalobos^{‡2}

From the [‡]Institute of Molecular Biology and Genetics, University of Valladolid and Spanish Research Council, 47003 Valladolid, Spain and the [§]Department of Biophysics, University of Saarland, 66421 Homburg, Germany

Abnormal vascular smooth muscle cell (VSMC) proliferation contributes to occlusive and proliferative disorders of the vessel wall. Salicylate and other nonsteroidal anti-inflammatory drugs (NSAIDs) inhibit VSMC proliferation by an unknown mechanism unrelated to anti-inflammatory activity. In search for this mechanism, we have studied the effects of salicylate and other NSAIDs on subcellular Ca^{2+} homeostasis and Ca^{2+} -dependent cell proliferation in rat aortic A10 cells, a model of neointimal VSMCs. We found that A10 cells displayed both store-operated Ca^{2+} entry (SOCE) and voltage-operated Ca^{2+} entry (VOCE), the former being more important quantitatively than the latter. Inhibition of SOCE by specific Ca^{2+} released-activated Ca^{2+} (CRAC/Orai) channels antagonists prevented A10 cell proliferation. Salicylate and other NSAIDs, including ibuprofen, indomethacin, and sulindac, inhibited SOCE and thereby Ca^{2+} -dependent, A10 cell proliferation. SOCE, but not VOCE, induced mitochondrial Ca^{2+} uptake in A10 cells, and mitochondrial depolarization prevented SOCE, thus suggesting that mitochondrial Ca^{2+} uptake controls SOCE (but not VOCE) in A10 cells. NSAIDs depolarized mitochondria and prevented mitochondrial Ca^{2+} uptake, suggesting that they favor the Ca^{2+} -dependent inactivation of CRAC/Orai channels. NSAIDs also inhibited SOCE in rat basophilic leukemia cells where mitochondrial control of CRAC/Orai is well established. NSAIDs accelerate slow inactivation of CRAC currents in rat basophilic leukemia cells under weak Ca^{2+} buffering conditions but not in strong Ca^{2+} buffer, thus excluding that NSAIDs inhibit SOCE directly. Taken together, our results indicate that NSAIDs inhibit VSMC proliferation by facilitating the Ca^{2+} -dependent inactivation of CRAC/Orai channels which normally is prevented by mitochondria clearing of entering Ca^{2+} .

Increased vascular smooth muscle cell (VSMC)³ proliferation, a process controlled by Ca^{2+} channel switching, is a key event in the development of atherosclerosis, restenosis, and other occlusive and proliferative disorders of the vasculature (1, 2). Salicylate, the major aspirin metabolite, and other nonsteroidal anti-inflammatory drugs (NSAIDs) may induce direct, platelet-independent effects on the vascular wall (3–5). For example, salicylate effectively inhibits VSMC proliferation and DNA synthesis *in vivo* and *in vitro* without inducing cellular toxicity or apoptosis (4).

A series of NSAIDs, including aspirin, ibuprofen, indomethacin, and sulindac, induce a dose-dependent inhibition of proliferation in A10 cells (6, 7), a VSMC cell line derived from embryonic rat aorta. The effects of NSAIDs occur in the absence of cytotoxicity and are independent of cyclooxygenase (7). Aspirin treatment also inhibits neointimal proliferation in dogs fed a cholesterol-enriched diet (8) and prevents the development of atherosclerosis in rabbits (9). Therefore, NSAIDs inhibit VSMC proliferation and show salutary effects in the treatment of vascular proliferative disorders by a yet unknown mechanism of action unrelated to anti-inflammatory activity.

Intracellular Ca^{2+} is a major trigger for vasoconstriction and a stimulus for VSMC proliferation (1, 2, 10). Several Ca^{2+} channels participate in regulating intracellular Ca^{2+} , including voltage-operated and store-operated Ca^{2+} channels (10, 11). SOCE is activated after the emptying of intracellular Ca^{2+} stores by physiological stimuli and is involved in cell proliferation in several cell types, including T cells (12, 13). In these cells, SOCE requires not only the activating signal from the empty store but also the close proximity of functional mitochondria acting as Ca^{2+} sinks to prevent the strong Ca^{2+} -dependent inactivation of SOC channels (14–18). It is unknown whether mitochondria control SOCE in VSMCs or not. Recently, two important pro-

* This work was supported by Grants SAN191/VA1806, CSI12A08 from Junta de Castilla y León, Spain, BFU2009-0867 from Ministerio de Ciencia e Innovación, Spain, and PI07/0766 from Instituto de Salud Carlos III, Spain, and Deutsche Forschungsgemeinschaft Grant A3 in the Sonderforschungsbereich 530.

[§] The on-line version of this article (available at <http://www.jbc.org>) contains supplemental Figs. 1–6.

¹ Present address: Harvard University School of Medicine, Boston, MA 02115.

² To whom correspondence should be addressed. Fax: 34-983-184800; E-mail: carlosv@ibgm.uva.es.

³ The abbreviations used are: VSMC, vascular smooth muscle cell; 2-APB, 2-aminoethoxydiphenyl borate; BTP2, *N*-(4-[3,5-bis(trifluoromethyl)-1H-pyrazol-1-yl]phenyl)-4-methyl-1,2,3-thiadiazole-5-carboxamide; $[\text{Ca}^{2+}]_{\text{cyt}}$, cytosolic Ca^{2+} concentration; $[\text{Ca}^{2+}]_{\text{mit}}$, mitochondrial Ca^{2+} concentration; CCCP, carbonyl cyanide *p*-chlorophenylhydrazone; Icrac, Ca^{2+} -release activated current; $\Delta\psi$, mitochondrial potential; FCCP, carbonyl cyanide-*p*-trifluoromethoxyphenylhydrazone; NSAID, nonsteroidal anti-inflammatory drug; RBL, rat basophilic leukemia; SOCE, store-operated Ca^{2+} entry; TMRM, tetramethyl rhodamine methyl ester; VOCE, voltage-operated Ca^{2+} entry.

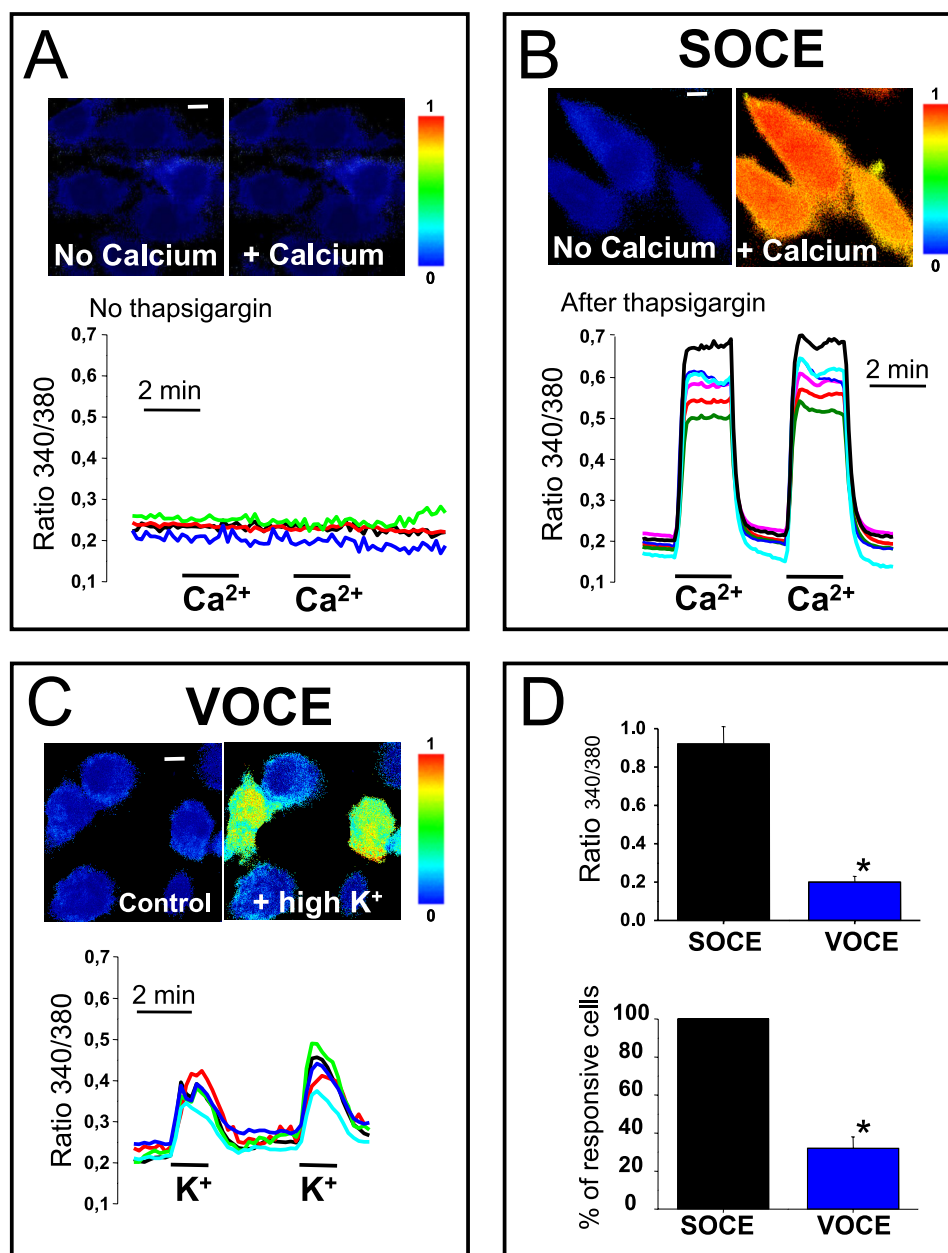


FIGURE 1. **A10 cells show SOCE and VOCE.** A10 cells were loaded with Fura-2/AM and subjected to fluorescence imaging of cytosolic Ca²⁺. **A**, in intact cells the addition of extracellular Ca²⁺ does not change the ratio of fluorescences excited at 340 and 380 nm (*Ratio 340/380*) reflecting [Ca²⁺]_{cyt}. **B**, in thapsigargin-treated cells, readdition of Ca²⁺ increased this ratio in all cells ($n = 5$ experiments) reflecting SOCE. A further Ca²⁺ pulse evoked the same response. Pictures on top show representative ratio images (from 0 to 1) coded in pseudocolor. **C**, depolarization with medium containing a high concentration (75 mM) of K⁺ (in exchange for Na⁺) induced a lower increase in the ratio in a fraction of cells revealing VOCE ($n = 3$ experiments). **D**, top bars show the size of rise in ratio induced by SOCE and VOCE in responsive cells. Bottom bars show percent of cells showing SOCE and VOCE, respectively (mean \pm S.E. (error bars), *, $p < 0.05$).

teins involved in SOCE have been discovered: Stim1, a sensor of the Ca²⁺ content of the store (19), and Orai1, a plasma membrane store-operated Ca²⁺ channel (20). Both proteins have been recently involved in SOCE in VSMCs (21–25) although other proteins, including members of the TRPC family of cation channels, might be involved in SOCE as well (26–28). SOCE and the novel proteins Stim1 and Orai1 may be involved in VSMC proliferation *in vitro* and *in vivo*. Knockdown of Stim1 decreases SOCE, inhibits cAMP response element-binding protein transcription factor activation, and prevents human coronary artery VSMC proliferation (25, 29).

Ca²⁺ handling is altered when arterial myocytes progress from a contractile to a proliferative phenotype. In the proliferative phenotype, the cells show increased SOCE, and Stim and Orai proteins are up-regulated (30). Furthermore, proliferating arterial myocytes have up-regulated Stim1, and its knockdown prevents nuclear factor of activated T cell-dependent transcription activity and growth factor-induced proliferation (31). Stim1 knockdown also prevents neointima formation and restenosis in animal models of injured carotid artery (31, 32). Rat aortic VSMCs display a SOC quite similar to the classic Ca²⁺ release-activated Ca²⁺ current (I_{crac}; 33), and the knockdown

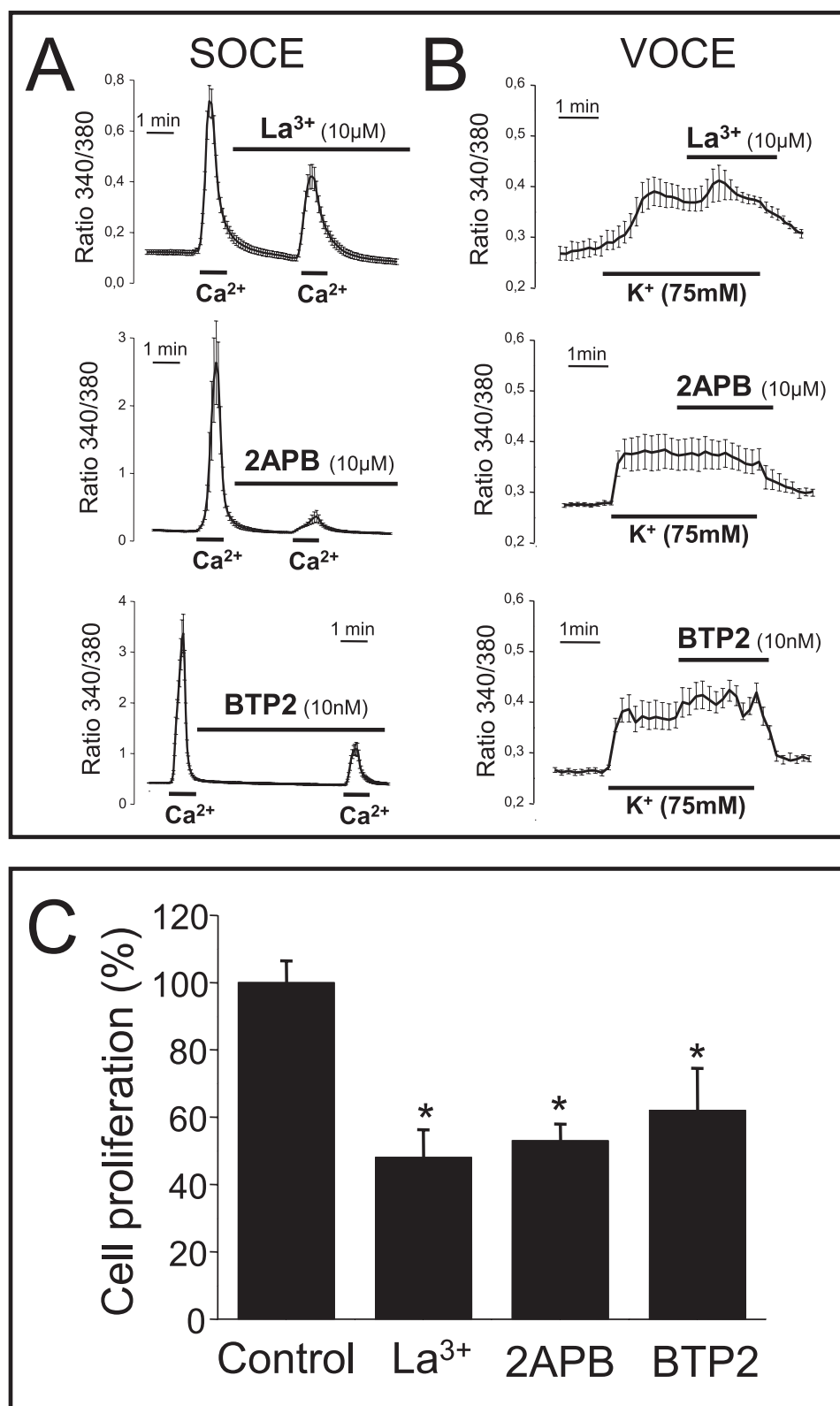


FIGURE 2. **SOCE antagonists inhibit A10 cell proliferation.** *A*, SOCE measurements were carried out as in Fig. 1. *Panel*s show representative experiments for each antagonist tested. Average (mean ± S.E. (error bars)) recordings of all cells in the same fields ($n = 7-9$ cells) are shown ($n = 3$). *B*, effects of antagonists on VOCE were investigated as in Fig. 1. Antagonists were added at the indicated concentrations after depolarization ($n = 3$). *C*, A10 cells were cultured for 15 days *in vitro*, and the effects of antagonists on cell proliferation were tested. La³⁺ and 2-APB were used at 10 μM and BTP2 at 10 nM (*, $p < 0.05$ versus control, $n = 3$). Antagonists had no effect on cell viability (data not shown).

of either Stim1 or Orai1 (but not Orai2, Orai3, TRPC1, 4, or 6) inhibits SOCE, Icrac, and VSMC proliferation and migration (29). Thus, Orai1- and Stim1-dependent SOCE may play an important role in VSMC proliferation. It is not surprising, therefore, that these proteins have been proposed as candidate targets for proliferative disorders of the vascular wall (31, 32).

We have investigated whether salicylate and other NSAIDs might prevent VSMC proliferation acting on signals controlling SOCE activity. First, we have characterized SOCE and its contribution to cell proliferation in A10 rat aortic cells, a model of neointimal VSMCs (34). Second, we have asked whether NSAIDs prevent A10 cell proliferation acting on SOCE. Finally, the possible mechanism of SOCE inhibition was investigated.

EXPERIMENTAL PROCEDURES

Materials—Fura-2/AM, tetramethyl rhodamine methyl ester (TMRM), and coelenterazines are from Invitrogen. LaCl₃, *N*-(4-[3,5-bis(trifluoromethyl)-1H-pyrazol-1-yl]phenyl)-4-methyl-1,2,3-thiadiazole-5-carboxamide (BTP2), and 2-aminoethoxydiphenyl borate (2-APB) are from Calbiochem. Thapsigargin and nifedipine are from Alomone Labs (Jerusalem, Israel). Media and sera are from Lonza (Basel, Switzerland). Other chemicals are from Sigma-Aldrich or Merck. Mitochondria-targeted GFP-aequorin and A10 cells were kindly donated by Profs. Philippe Brulet (CNRS, Paris, France) and Santiago Lamas (Consejo Superior de Investigaciones Científicas, Madrid, Spain), respectively.

Cell Culture—A10 cells were cultured in Dulbecco's modified Eagle's medium (DMEM) supplemented with glutamine and antibiotics. RBL-2H3 cells were cultured in MEM- α (Invitrogen, 22561-021) supplemented with 15% fetal bovine serum (FBS; Invitrogen, 10270-106), 1% GlutaMAX (Invitrogen, 35050-038) and 1% PenStrep (Invitrogen, 15140-122), which contains 10,000 units/ml penicillin and 10,000 μ g/ml streptomycin. Cells were maintained continuously in log-phase growth at 37 °C with 5% CO₂. Cells were prepared at a concentration of 3000 cells/well 24–48 h before patch clamp and imaging experiments.

Store-operated and Voltage-operated Ca²⁺ Entry—SOCE was monitored as reported earlier (35) by imaging the rise in cytosolic Ca²⁺ concentration ([Ca²⁺]_{cyt}) that follows Ca²⁺ addition to cells with depleted Ca²⁺ stores. VOCE was measured by imaging the rise in [Ca²⁺]_{cyt} induced by depolarization with high K⁺ (75 mM) instead of Na⁺. A10 cells were plated at about 17 × 10⁴ cells/ml (10 × 10³ cells/60 μ l) on 12-mm glass coverslips coated with 0.01 mg/ml poly-L-lysine. After 24 h, cells were loaded with 4 μ M Fura-2/AM for 1 h at room temperature, incubated with thapsigargin (1 μ M) for 10 min in Ca²⁺-free medium containing 145 mM NaCl, 5 mM KCl, 1 mM MgCl₂, 0.5 mM EGTA, 10 mM glucose, 10 mM Hepes/NaOH, pH 7.42, and placed on the stage of an inverted microscope (Zeiss Axiovert S100 TV). Subsequently, cells were perfused with pre-warmed (37 °C) Ca²⁺-free medium and illuminated alternately at 340 and 380 nm before test solutions. Light emitted at wavelengths longer than 520 nm was recorded with a Hamamatsu OrcaER digital camera through a 40 × oil lens (NA 1.3). Pixel-by-pixel ratios of consecutive frames were captured and analyzed using the Aquacosmos® software.

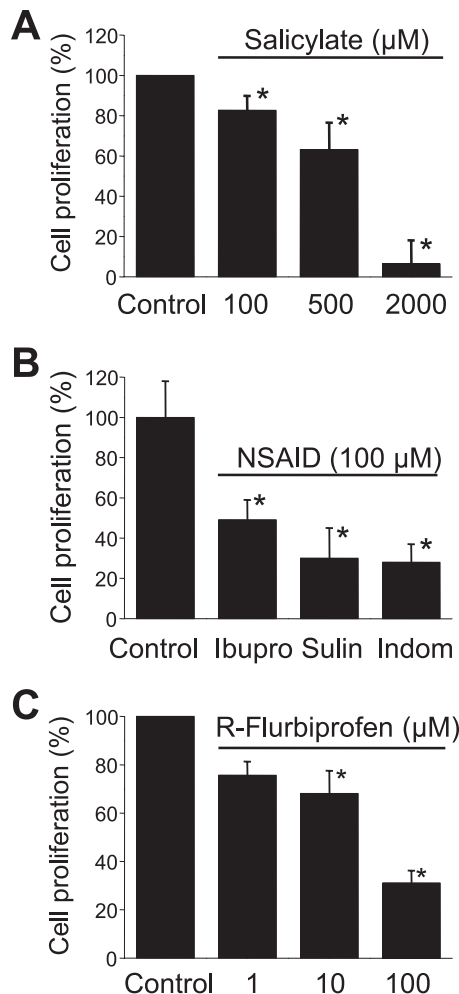


FIGURE 3. NSAIDs inhibit A10 cell proliferation. *A*, dose-dependent effects of salicylate (100–2000 μ M) on A10 cell proliferation. *B*, effects of different NSAIDs including ibuprofen, sulindac, and indomethacin, all tested at 100 μ M, on A10 cell proliferation. *C*, dose-dependent effects of (*R*)-flurbiprofen (1–100 μ M) on A10 cell proliferation. *, $p < 0.05$ versus control ($n = 3$). Results are mean \pm S.E. (error bars).

Electrophysiology—Patch clamp experiments were performed in the tight seal whole cell configuration at 21–25 °C. Membrane currents were acquired with an EPC-9 patch clamp amplifier (HEKA). Voltage ramps of 200-ms duration spanning a range of –150 to +100 mV were delivered from a holding potential of 0 mV at a rate of 0.5 Hz over a period of 400 s. All voltages were corrected for a liquid junction potential of –12 mV between internal and bath solutions. Currents were filtered at 2.9 kHz and digitalized at a sampling rate of 10 kHz. To display the current recordings, currents were digitally filtered offline at 1 kHz. Pipette and cell capacitance were electronically canceled before each voltage ramp. Current amplitudes at –130 mV from individual voltage ramp current were used to depict the temporal development of currents and analyze current inactivation. Statistical errors of averaged data are given as means \pm S.E. analyzing n cells. Standard external solution was as follows: 120 mM NaCl, 2 mM MgCl₂, 10 mM CaCl₂, 10 mM Tetraethylammonium-Cl, 10 mM Hepes, 10 mM glucose, pH 7.2 with NaOH, 300 mosmol liter⁻¹. Ibuprofen, indomethacin, and salicylate were added to the external solution at a final concen-

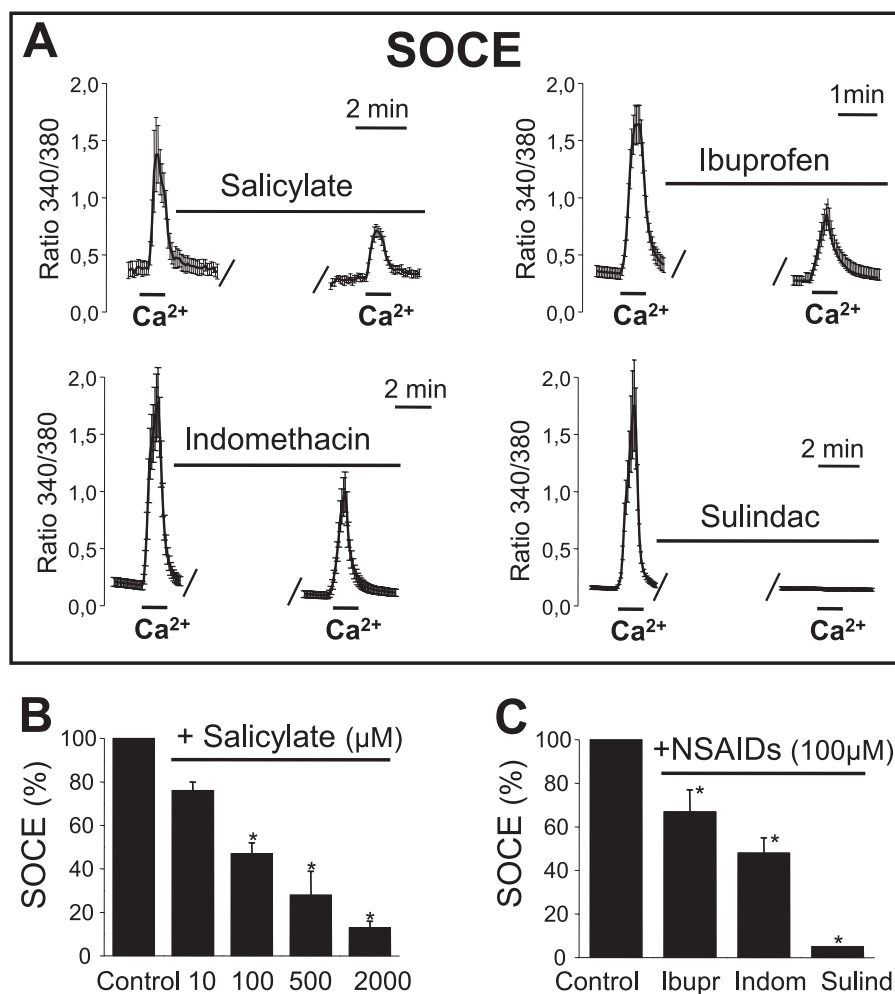


FIGURE 4. NSAIDs inhibit SOCE in A10 cells. SOCE was measured in A10 cells as in Fig. 1. *A*, Ca²⁺ recordings are mean ± S.E. (error bars; *n* = 9,9,18 cells, respectively) and representative of *n* = 3. *B*, bars show the dose-dependent effects of salicylate on SOCE (mean ± S.E. values, *n* = 3). *C*, bars show the effects of ibuprofen, indomethacin, and sulindac, all tested at 100 μM, on SOCE. *, *p* < 0.05.

tration of 10 and 100 μM. Cells were preincubated with each compound for 5 min before patching them. The standard pipette solution for whole cell patch clamp recordings contained 0.05 mM inositol trisphosphate, 5 × 10⁻⁸ mM thapsigargin, 120 mM Cs-glutamate, 8 mM NaCl, 10 mM Cs-BAPTA, 3 mM MgCl₂, 4 mM CaCl₂, 10 mM Hepes, pH 7.2 with CsOH, 300 mM mosmol liter⁻¹ (resulting in 150 nM free Ca²⁺ as calculated with WebMaxC). To weakly buffer Ca²⁺ in the pipette, the following solution was used: 1.2 mM EGTA, 0.05 mM inositol trisphosphate, 5 × 10⁻⁸ mM thapsigargin, 145 mM Cs-aspartate, 3 mM MgCl₂, 8 mM NaCl, 10 mM Cs-Hepes, pH 7.2 with CsOH, 280 mosmol liter⁻¹. The mitochondrial mixture to preserve mitochondrial respiration contained 5 mM Mg-ATP, 0.5 mM Tris-GTP, 2.5 mM malic acid, 2.5 mM Na⁺-pyruvate, 1 mM NaH₂PO₄. The mitochondrial mixture was added to the weak Ca²⁺ buffer solution just before starting the experiment. Data were analyzed using Igor Pro (Wavemetrics), Pulse (HEKA), FitMaster (HEKA), and Excel (Microsoft). All values are given as mean ± S.E. (number of cells). Three or more independent experiments were performed for each experimental condition. In case, data points were normally distributed, an unpaired two-sided Student's *t* test was used. If normal distribution could

not be confirmed, a nonparameterized test (Mann-Whitney) was carried out. *p* values are stated in the figure legends.

RT-PCR—Total RNA was extracted from A10 cells using TRIzol reagent (Invitrogen). cDNA was made from 2 μg of RNA by a high capacity cDNA Reverse Transcription kit (Applied Biosystems). The sense and antisense primers targeting Stim1 and Orai1 were designed using PRIMER 3 software. PCR was performed by using the following primers: rat Stim1 sense, 5'-TAA CTG GAC CGT GGA TGA GG-3' and antisense, 3'-GTC CAC TAA CAC CGC TCA G-5'; rat Orai1 sense, 5'-TGG TAG CGA TGG TGG AAG TC-3' and antisense 3'-TGC CTC AAC TCC AAC ACC TG-5'. Primers were synthesized by VWR International Eurolab (Barcelona, Spain). Amplification was started with initial denaturation at 94 °C for 3 min, then 25–30 cycles with denaturation at 94 °C for 60 s, annealing at 60 °C for 1 min, and extension at 72 °C for 30 s and was followed by a final extension at 72 °C for 10 min. Gel electrophoresis was used to identify the PCR products in a 1% agarose gel using ethidium bromide staining.

Cell Proliferation—Cells were cultured in DMEM containing 10% FBS and antibiotics. Cells were plated in wells at about 10 × 10³ in 3 ml and incubated with test solutions for 15 days.

Cell number was determined at day 1 and at day 15 using a hemocytometer. Cell death was estimated using trypan blue staining.

Mitochondrial Potential ($\Delta\psi$)—A10 cells were loaded with the $\Delta\psi$ probe TMRM (100 nM) for 30 min at room temperature, placed on the perfusion chamber of a Zeiss Axiovert S100 TV inverted microscope and superfused continuously with pre-warmed (37 °C) standard medium. Fluorescence images were taken at 10-s intervals with a Hamamatsu OrcaER camera. At the end of the recording, the mitochondrial uncoupler carbonyl cyanide-*p*-trifluoromethoxyphenylhydrazone (FCCP, 10 μ M) was perfused for 5 min to collapse $\Delta\psi$. The fluorescence image of TMRM after collapse of $\Delta\psi$ was used as background fluorescence in conditions of total uncoupling. Fluorescence recordings from individual cells were expressed as the percent value of the value just before treatment and averaged as reported previously (36).

Bioluminescence Imaging of Mitochondrial Ca^{2+} —A10 cells were nucleofected (Amaxa) with a plasmid containing mitochondria-targeted, GFP-aequorin. 24 h later, cells were incubated in standard medium (see above) containing 4 μ M coelenterazine h or n for 2 h at room temperature. Then, the coverslips were placed in the stage of an inverted microscope (Zeiss Axiovert S100 TV) equipped with a bottom-port attached, Hamamatsu VIM photon counting camera handled with an Argus 20 image and the Aquacosmos® software. Cells were perfused continuously with warm (37 °C) standard medium and subjected to photon counting imaging at 10-s intervals. For experiments in intact cells, cells were perfused with standard medium. The effects of SOCE on $[Ca^{2+}]_{mit}$ were imaged after presentation of 1 mM extracellular Ca^{2+} to cells previously treated with thapsigargin in Ca^{2+} -free medium. The effects of VOCE on $[Ca^{2+}]_{mit}$ were imaged after depolarization with high K^+ medium. For experiments in permeated cells, A10 cells were permeated with 20 μ M digitonin in “intracellular” medium (130 mM KCl, 10 mM NaCl, 1 mM $MgCl_2$, 1 mM K_3PO_4 , 0.2 mM EGTA, 1 mM ATP, 20 μ M ADP, 2 mM succinate, 20 mM HEPES/KOH, pH 6.8). Then, the cells were incubated with the same medium containing 200 nM Ca^{2+} (buffered with EGTA) with or without NSAIDs for 5 min. Finally, perfusion was switched to “intracellular” medium containing 10 μ M Ca^{2+} (with or without NSAIDs) for 1 min. Photonic emissions were converted to mitochondrial Ca^{2+} concentration ($[Ca^{2+}]_{mit}$) values as detailed elsewhere (37, 38).

Cell ATP Levels—Cells were seeded in 6-well plates and cultured in medium containing either vehicle or different NSAIDs. After 3 days, cells were washed twice with phosphate-buffered saline (PBS) at 37 °C, and 1 ml of boiling 20 mM Tris, pH 7.75, 4 mM EDTA solution was added. After 2 min, samples were centrifuged for 5 min at 10,000 \times g. ATP was measured later from the supernatant by the luciferin-luciferase assay using a Cairn luminometer (Cairn Research, Kent, UK).

Statistics—When only two means were compared, Student's *t* test was used. For >2 groups, statistical significance of the data was assessed by ANOVA and compared using Bonferroni's multiple comparison tests. Differences were considered significant at *p* < 0.05.

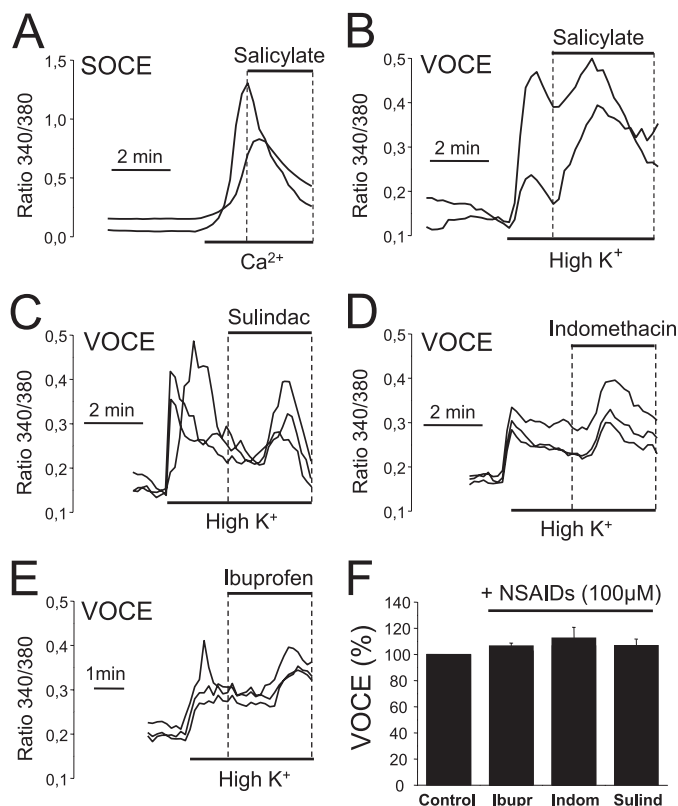


FIGURE 5. NSAIDs do not inhibit VOCE in A10 cells. SOCE was measured in A10 cells as in Fig. 1. *Panels* show Ca^{2+} recordings of individual cells in experiments representative of at least three similar ones. *A*, salicylate (500 μ M) decreases $[Ca^{2+}]_{cyt}$ after the Ca^{2+} readdition to thapsigargin-treated cells. *B–F*, effects of NSAIDs on VOCE were tested by recording the effect of NSAIDs perfused after depolarization with high K^+ medium. Neither 500 μ M salicylate (*B*), 100 μ M sulindac (*C*), 100 μ M indomethacin (*D*), nor 100 μ M ibuprofen decreased $[Ca^{2+}]_{cyt}$ when perfused during depolarization. *F* shows mean \pm S.E. (error bars) values of the levels of $[Ca^{2+}]_{cyt}$ before (control) and after NSAID treatment (*p* > 0.05, *n* = 3).

RESULTS

We have characterized SOCE in A10 rat aorta VSMCs. Fluorescence imaging experiments show that cells with intact Ca^{2+} stores (Fig. 1A) undergo no change in $[Ca^{2+}]_{cyt}$ when extracellular Ca^{2+} is added. However, cells with depleted stores displayed large increases in $[Ca^{2+}]_{cyt}$ after the addition of extracellular Ca^{2+} revealing SOCE. A second pulse induced a similar rise in $[Ca^{2+}]_{cyt}$ (Fig. 1B). Plasma membrane depolarization with medium containing a high K^+ concentration also increases $[Ca^{2+}]_{cyt}$ revealing VOCE (Fig. 1C). Interestingly, the relative abundance of cells showing Ca^{2+} entry and the size of the rise in $[Ca^{2+}]_{cyt}$ was larger for SOCE than for VOCE (Fig. 1D).

To characterize SOCE further in A10 cells and its role in cell proliferation, we investigated expression of Orai1 and Stim1, recently involved in SOCE in other cell types including VSMC (22–25). **Supplemental Fig. 1** shows that A10 cells expressed both Stim1 and Orai1 mRNAs as determined by RT-PCR. Second, the effects of a series of antagonists on SOCE and VOCE were tested in A10 cells. Fig. 2A shows that classic SOCE antagonists including $LaCl_3$ (La^{3+}) and 2-APB inhibited SOCE. BTP2, a novel Icrac antagonist (39), also inhibited SOCE but at a much lower concentration (Fig. 2A). SOCE antagonists did

CRAC/Orai Channels in NSAID Inhibition of VMSC Proliferation

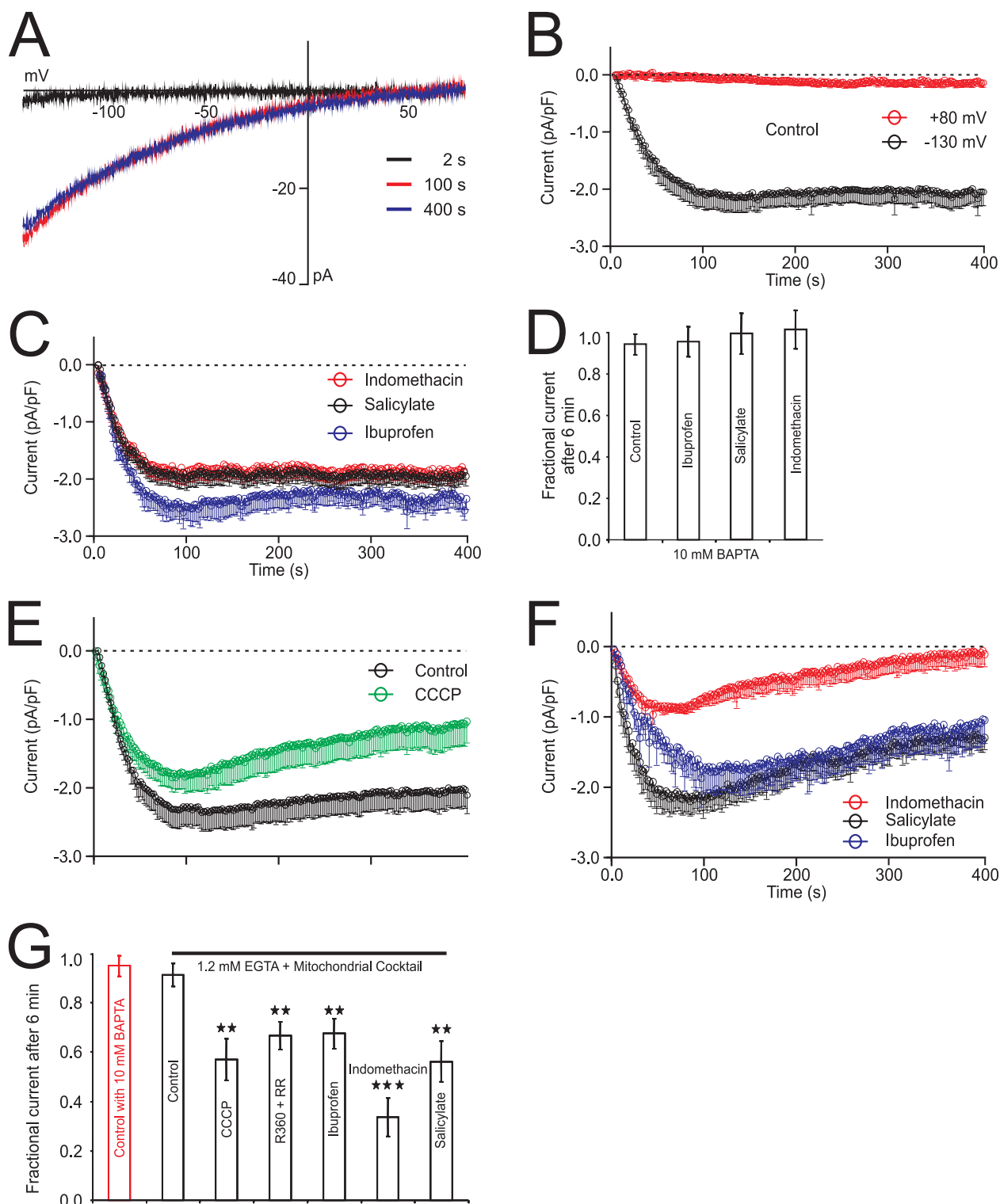


FIGURE 6. NSAIDs accelerate slow inactivation of CRAC currents in RBL cells under weak Ca^{2+} buffering conditions. *A–C*, average current-voltage (I/V) relationship of CRAC currents from RBL-2H3 cells patched with the strong buffer solution (10 mM BAPTA) at 2 (*black trace*), 100 (*red trace*), and 400 (*blue trace*) s after establishing the whole cell configuration and current kinetics in control cells (*B*, $n = 16$) and in cells exposed (*C*) to ibuprofen ($n = 7$), salicylate ($n = 11$), indomethacin ($n = 6$), all tested at 10–100 μM is shown. *D*, average CRAC currents were obtained from cells as shown in *B* and *C*, respectively. Currents sizes were extracted at -130 (*black trace*) and $+80$ (*red trace*) mV, normalized to the cell size, averaged, and plotted versus time. Currents were leak-corrected by subtracting averages of the currents from first three voltage ramps before CRAC channel activation. *E*, CRAC currents were studied in control cells with the weakly buffering solution (1.2 mM EGTA) and the mitochondrial mixture (see “Experimental Procedures”) except that cells were preincubated with CCCP for 5 min to disrupt mitochondrial Ca^{2+} uptake. *F*, same conditions were used as in *E* except that cells were preincubated with indomethacin (*red trace*), salicylate (*black trace*), or ibuprofen (*blue trace*). *G*, statistical analysis of CRAC currents was performed 6 min after establishing the whole cell configuration as a fraction of the maximal current for the control conditions and for experiments in the presence of R360 + RR. Levels of significance are indicated (**, $p < 0.01$; ***, $p < 0.001$). Error bars indicate S.E.

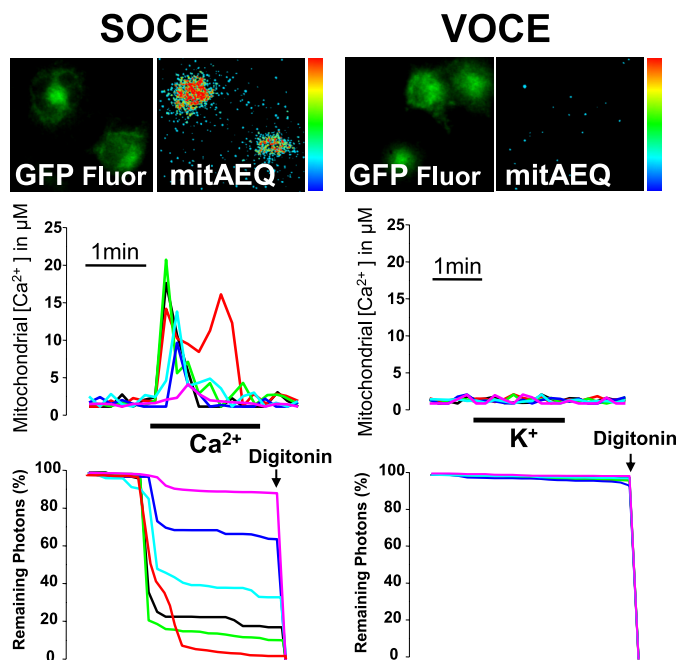


FIGURE 7. SOCE, but not VOCE, induces mitochondrial Ca^{2+} uptake in A10 cells. A10 cells were transfected with GFP-aequorin targeted to mitochondria, loaded with coelenterazine, and subjected to bioluminescence imaging of mitochondrial $[\text{Ca}^{2+}]$ in single cells. *Left* (SOCE), A10 cells were treated with $1 \mu\text{M}$ thapsigargin for 10 min in Ca^{2+} -free medium to deplete intracellular Ca^{2+} stores and perfused with extracellular Ca^{2+} containing medium to induce SOCE, and the effects on photonic emissions reflecting mitochondrial Ca^{2+} uptake were imaged. *Pictures on top* show a typical fluorescence image of transfected cells (*left*) and the accumulated photonic emissions during SOCE. *Top traces* show calculated $[\text{Ca}^{2+}]_{\text{mit}}$ values in individual cells. *Bottom traces* reflect percent of remaining photonic emissions. *Right* (VOCE), cells were perfused with high K^{+} -containing medium to induce VOCE, and the effects on photonic emissions reflecting mitochondrial Ca^{2+} uptake were imaged. *Top pictures* are representative fluorescence and bioluminescence images. *Traces* show $[\text{Ca}^{2+}]_{\text{mit}}$ recordings in individual cells and percent remaining counts. Data are representative of at least three independent experiments of each kind. *Pseudocolor scale* goes from 0 to 10 photons/pixel.

not inhibit VOCE in A10 cells (Fig. 2B), and dihydropyridines that block VOCE did not inhibit SOCE (supplemental Fig. 2). Third, we studied the effects of SOCE antagonists on A10 cell proliferation. La^{3+} , 2-APB, and BTP2 inhibited A10 cell proliferation at the same concentrations that prevent SOCE (Fig. 2C), consistent with a role for SOCE in A10 cell proliferation.

As reported above, salicylate and other NSAIDs show salutary effects in the vascular wall and prevent VSMC proliferation by a yet unknown mechanism unrelated to anti-inflammatory activity (3–9). Fig. 3 shows that salicylate inhibits A10 cell proliferation in a dose-dependent manner. Other NSAIDs, including ibuprofen, sulindac, and indomethacin, also inhibited A10 cell proliferation at therapeutic concentrations. (*R*)-flurbiprofen, an optic enantiomer lacking anti-inflammatory activity, inhibits A10 cell proliferation in a dose-dependent manner. In search for the anti-proliferative mechanism, we have investigated the effects of NSAIDs on SOCE in A10 cells. Salicylate, ibuprofen, indomethacin, and sulindac inhibited SOCE significantly in A10 cells (Fig. 4). Similar results were obtained with (*R*)-flurbiprofen (supplemental Fig. 3). Inhibition of SOCE by salicylate is also observed even when salicylate is added after the rise in $[\text{Ca}^{2+}]_{\text{cyt}}$ induced by Ca^{2+} pulse in store-depleted cells (Fig. 5A). NSAIDs could inhibit A10 cell proliferation acting

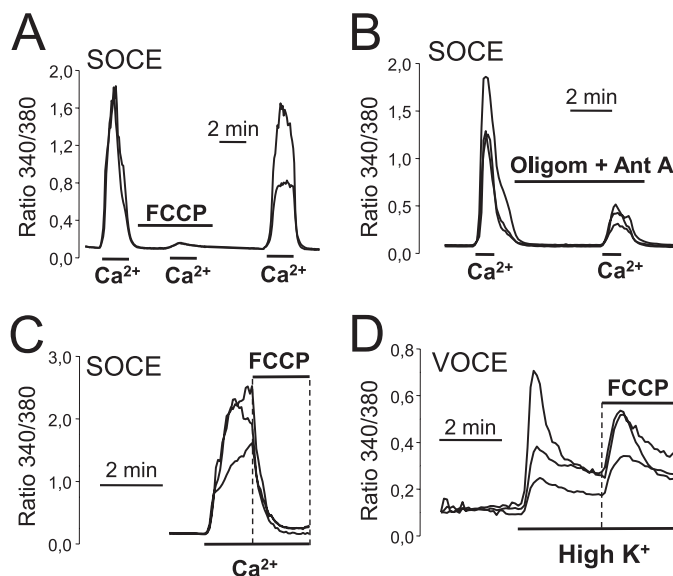


FIGURE 8. Mitochondrial depolarization inhibits SOCE but not VOCE in A10 cells. SOCE was estimated in A10 cells as shown in Fig. 1. *A*, $10 \mu\text{M}$ FCCP (added in the presence of $0.12 \mu\text{M}$ oligomycin) inhibits SOCE in a reversible manner. *B*, mitochondrial depolarization with antimycin A ($0.5 \mu\text{g/ml}$) + oligomycin ($0.12 \mu\text{M}$) also inhibits SOCE in A10 cells. *C*, $10 \mu\text{M}$ FCCP added during SOCE decreases $[\text{Ca}^{2+}]_{\text{cyt}}$. *D*, FCCP added after depolarization with high K^{+} did not decrease $[\text{Ca}^{2+}]_{\text{cyt}}$, but rather increased it. All data are single-cell recordings representative of 8–17 cells studied in at least three independent experiments for each panel.

also on VOCE. However, none of the NSAIDs tested inhibited VOCE in A10 cells (Fig. 5, B–F). Interestingly, the addition of NSAIDs during the depolarizing pulse promoted rather a small rise in $[\text{Ca}^{2+}]_{\text{cyt}}$. Thus, NSAIDs inhibit Ca^{2+} -dependent cell proliferation in A10 cells acting on SOCE but not on VOCE. Consistent with the role of Ca^{2+} entry in proliferation, chelating extracellular Ca^{2+} also largely inhibited A10 cell proliferation whereas the equimolar addition of excess Ca^{2+} did not inhibit proliferation, indicating that EGTA had no toxic effects (supplemental Fig. 4). In addition, an NSAID (indomethacin) inhibited Ca^{2+} -dependent proliferation but had no further effect in the absence of extracellular Ca^{2+} (supplemental Fig. 4).

NSAIDs may inhibit SOCE acting directly on CRAC channels or modulating a SOCE regulatory mechanism. To address this issue we have investigated the effects of NSAIDs on Icrac in RBL cells. We used RBL cells for two reasons. First, Icrac is large and well characterized in these cells (15). Second, a strong mechanism of regulation of Icrac and SOCE by mitochondria in RBL cells is also well characterized (15, 16). Consistently, we found that RBL cells displayed a robust SOCE that was nearly abolished by mitochondrial uncoupling (supplemental Fig. 5). We tested the effects of salicylate, ibuprofen, indomethacin, and sulindac on SOCE in RBL cells. We found that all tested NSAIDs inhibited SOCE in RBL cells just as they did in A10 cells (supplemental Fig. 5). Next, we tested the effects of NSAIDs on CRAC/Orai channel activity in RBL cells directly using the whole cell patch clamp configuration. Fig. 6 shows the typical inward rectifying *I-V* relationship for Icrac at 2, 100, and 400 s after starting recording in control cells. Neither salicylate, ibuprofen, nor indomethacin inhibited Icrac in RBL cells studied under conditions of strong Ca^{2+} buffering (10 mM BAPTA). Under this condition, the inflowing Ca^{2+} is rapidly buffered by

CRAC/Orai Channels in NSAID Inhibition of VMSC Proliferation

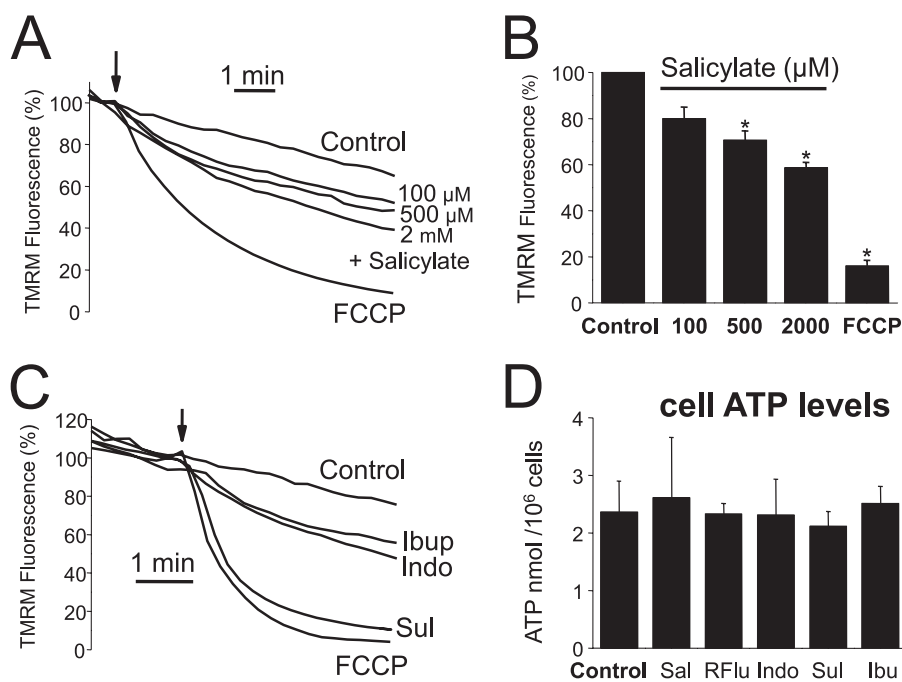


FIGURE 9. NSAIDs depolarize mitochondria in A10 cells. The effects of NSAIDs on mitochondrial potential were tested by fluorescence microscopy of cells loaded with TMRM. *A*, effects of vehicle, salicylate (100–2000 μM), or FCCP (10 μM) on TMRM fluorescence were normalized to the value before addition of treatment and averaged (arrow). *B*, mean \pm S.E. (error bars) values of three independent experiments are shown (*, $p < 0.05$). *C*, effects of vehicle (control), FCCP (10 μM), ibuprofen, indomethacin, and sulindac (all tested at 100 μM) on TMRM fluorescence were normalized to the value before addition of treatment (arrow). Results are representative of $n = 3$ experiments. *D*, effects of NSAIDs including salicylate, (*R*)-flurbiprofen, indomethacin, sulindac sulfide, and ibuprofen on ATP levels in A10 cell are shown. All NSAIDs were tested at 100 μM except salicylate which was tested at 500 μM . None of the treatments changed cell ATP levels in A10 cells ($n = 3$, $p > 0.05$).

the Ca^{2+} chelator and thereby reducing the Ca^{2+} -dependent channel inactivation efficiently (Fig. 6, *B* and *C*). The statistical analysis shows that in these conditions NSAIDs have no direct effects on CRAC/Orai channel activity (Fig. 6*D*). However, under weak Ca^{2+} buffering condition (1.2 mM EGTA), mitochondrial Ca^{2+} uptake has been reported to be essential for reducing the accumulation of incoming Ca^{2+} close to sites that govern Ca^{2+} -dependent CRAC channel inactivation (14–16). Indeed, mitochondrial depolarization induces significantly inhibition of Icrac (13–16). To keep the capability of mitochondria to take up Ca^{2+} during Icrac recording, a mixture of several compounds was supplied to the pipette solution (see “Experimental Procedures”). This mitochondrial mixture help to maintain the $\Delta\psi$ and the subsequent long lasting activity of CRAC/Orai channel activity. Fig. 6*E* shows the time course of Icrac in weak Ca^{2+} buffer in the presence of mitochondrial mixture. However, in presence of protonophore CCCP or specific mitochondrial uniporter blockers ruthenium red or ruthenium 360, the long lasting Icrac in cells dialyzed with mixture was significantly reduced (Fig. 6*E*). The same is true for indomethacin-, salicylate-, and ibuprofen-treated cells (Fig. 6*F*). Thus, only under weak Ca^{2+} buffering condition is CRAC significantly prevented by the uncoupler CCCP, ruthenium derivatives, and NSAIDs (Fig. 6*G*).

The above observations provide important clues regarding the mechanism of inhibition of SOCE by NSAIDs. They suggest that NSAIDs promote the Ca^{2+} -dependent inactivation of CRAC channels by preventing the ability of mitochondria to take up Ca^{2+} . To test this possibility we have investigated whether mitochondria controls SOCE in A10 cells just as they

do in Jurkat T and RBL cells (13–16). In the first place we studied whether Ca^{2+} entry induced by SOCE induces mitochondrial Ca^{2+} uptake. For this end, A10 cells were transfected with mitochondria-targeted aequorin and subjected to bioluminescence imaging for monitoring of $[\text{Ca}^{2+}]_{\text{mit}}$. Fig. 7*A* shows that Ca^{2+} pulses to cells with depleted stores induced a rise in $[\text{Ca}^{2+}]_{\text{mit}}$, indicating that mitochondria are sensitive to rises in $[\text{Ca}^{2+}]_{\text{cyt}}$ induced by SOCE. However, depolarization with high K^{+} failed to increase $[\text{Ca}^{2+}]_{\text{mit}}$ in any of the A10 cells tested (Fig. 7*B*). These data suggest, but do not prove, that mitochondria are not sensitive to $[\text{Ca}^{2+}]_{\text{cyt}}$ rises induced by VOCE in A10 cells. This effect is probably due to the low rise in $[\text{Ca}^{2+}]_{\text{cyt}}$ induced by VOCE (Fig. 1). Next, we investigated the effects of mitochondrial depolarization on SOCE. Fig. 8*A* shows that $\Delta\psi$ collapse induced by FCCP (+oligomycin) inhibits SOCE in a reversible manner in A10 cells. Similar results were obtained with antimycin A (+oligomycin) to depolarize mitochondria (Fig. 8*B*). Salicylate did not increase the effect of FCCP on SOCE further (supplemental Fig. 6), indicating that both FCCP and NSAID act by the same mechanism. FCCP also decreased SOCE when presented after Ca^{2+} readdition (Fig. 8*C*). Interestingly, addition of FCCP after depolarization with high K^{+} induced a small rise in $[\text{Ca}^{2+}]_{\text{cyt}}$, a behavior resembling the effects of NSAIDs (Fig. 5). Thus, mitochondrial uncoupling or depolarization inhibits SOCE but not VOCE in A10 cells.

To support further the view that NSAIDs inhibit SOCE acting on a mitochondria-dependent regulatory mechanism, we tested the effects of NSAIDs on $\Delta\psi$. Fig. 9, *A* and *B*, shows that salicylate decreases $\Delta\psi$ in A10 cells in a dose-dependent manner. Similar results were obtained with ibuprofen, sulindac, and

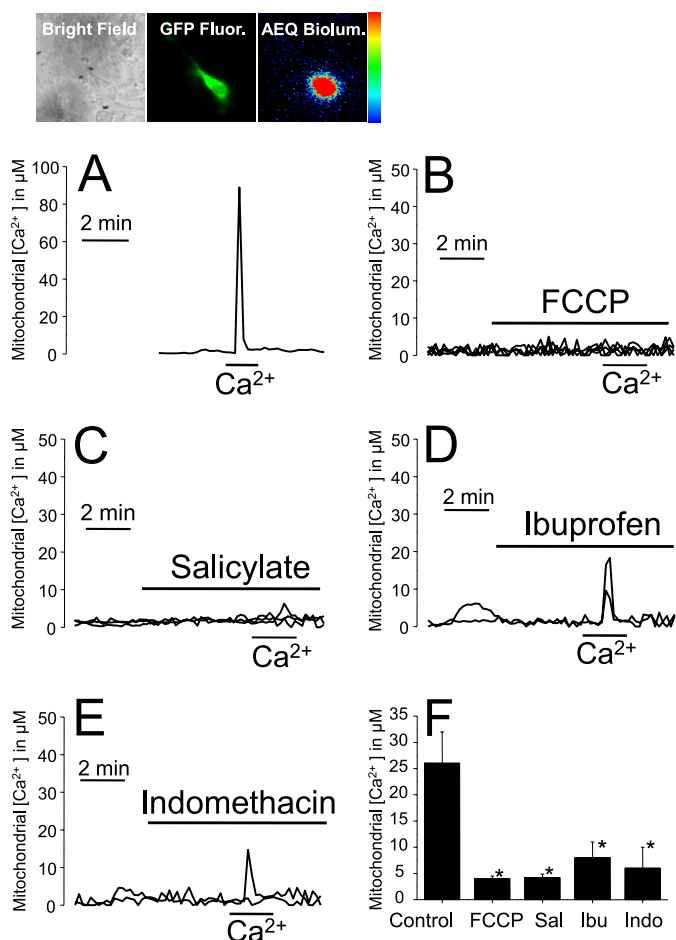


FIGURE 10. NSAIDs inhibit mitochondrial Ca^{2+} uptake in permeated A10 cells. A10 cells were transfected with GFP-aequorin targeted to mitochondria and subjected to bioluminescence counting imaging to estimate mitochondrial Ca^{2+} uptake in permeated, single cells. Pictures show a typical brightfield image, the GFP fluorescence image (*GFP Fluor.*), and photonic emissions released after a Ca^{2+} pulse (*AEQ Biolum.*). Cells were permeated with low concentrations of digitonin in internal medium. *A*, perfusion with internal medium containing $10 \mu\text{M}$ Ca^{2+} induced a large rise in $[\text{Ca}^{2+}]_{\text{mit}}$. *B*, $10 \mu\text{M}$ FCCP abolished the rise in $[\text{Ca}^{2+}]_{\text{mit}}$ induced by $10 \mu\text{M}$ Ca^{2+} . *C–E*, salicylate (*C*, $500 \mu\text{M}$), ibuprofen (*D*, $100 \mu\text{M}$), and indomethacin (*E*, $100 \mu\text{M}$) also inhibited $[\text{Ca}^{2+}]_{\text{mit}}$ rises induced by $10 \mu\text{M}$ Ca^{2+} . *Traces* are recordings representative of 4–7 cells studied in at least three independent experiments. *F*, bars show mean \pm S.E. (error bars) values of $[\text{Ca}^{2+}]_{\text{mit}}$ increases ($n = 3$; $p < 0.05$).

indomethacin at the same concentrations that inhibit SOCE and cell proliferation (Fig. 9C). To exclude any possible metabolic influence, we studied the effects of NSAIDs on cell ATP levels in A10 cells. Fig. 9D shows that treatment with NSAIDs did not affect the cell ATP levels significantly. Because $\Delta\psi$ is the driving force for mitochondrial Ca^{2+} uptake, we investigated next whether changes in $\Delta\psi$ induced by NSAIDs were sufficient to inhibit mitochondrial Ca^{2+} uptake. Toward this end, A10 cells were transfected with an aequorin plasmid fused to the GFP and targeted to mitochondria (37). After 24 h, cells were incubated with coelenterazine and subjected to photon-counting imaging for monitoring $[\text{Ca}^{2+}]_{\text{mit}}$ in individual A10 VSMCs. Transfected cells were selected by their GFP fluorescence (Fig. 10) where increases in $[\text{Ca}^{2+}]_{\text{mit}}$ promote the release of photonic emissions. Transfected A10 cells were permeated with low concentrations of digitonin (34) and then stimulated with internal medium containing $10 \mu\text{M}$ Ca^{2+} to evoke a rise in

$[\text{Ca}^{2+}]_{\text{mit}}$ (Fig. 10A), which was prevented by FCCP (Fig. 10B). NSAIDs, including salicylate at $500 \mu\text{M}$ (Fig. 10C) and $100 \mu\text{M}$ ibuprofen (Fig. 10D) and indomethacin (Fig. 10E), also inhibited the rise in $[\text{Ca}^{2+}]_{\text{mit}}$ in permeated A10 cells in a significant manner (Fig. 10F).

DISCUSSION

We show that NSAIDs inhibit proliferation of rat aortic A10 cells, a model of neointimal VSMC, and that this effect is mediated by inhibition of SOCE, an important Ca^{2+} entry pathway involved in cell proliferation. We also show that NSAIDs do not inhibit SOCE directly acting on CRAC channels but target an important regulatory mechanism of SOCE by mitochondria. The results confirm the importance of SOCE in VSMC proliferation and provide an action mechanism for the antiproliferative and salutary effects of NSAIDs in the vasculature. In support of this view, we demonstrated first that A10 cells display both SOCE and VOCE, the former being quantitatively larger than the latter, consistent with a proliferative VSMC phenotype (1, 2). Interestingly, SOCE activation in VSMC favors immediate-early gene expression and growth whereas VOCE promotes rather VSMC differentiation (40). SOCE in A10 cells resembles the one best characterized in T and RBL cells in the following aspects: (i) It is prevented by classic SOCE antagonists La^{3+} and 2-APB and the novel antagonist BTP2, (ii) A10 cells express Orai1 and Stim1 recently involved in CRAC in other cell types including VSMCs, (iii) SOCE is important in A10 cell proliferation just as in T cell clonal expansion (13), and (iv) SOCE is tightly modulated by mitochondria because inhibition of mitochondrial Ca^{2+} uptake prevents this pathway. Thus, SOCE in A10 VSMCs is regulated by mitochondria and involved in cell proliferation.

Our data agree with recent reports indicating that SOCE and novel proteins Stim1 and Orai1 are critical in VSMC proliferation. For example, proliferating VSMCs show increased SOCE and up-regulated Stim and Orai proteins (30), and their knockdown decreases SOCE and cell proliferation in coronary artery VSMCs (25) and in rat aortic VSMCs (29). Orai and Stim knockdown prevents restenosis in rat injured carotid artery (32). Increased SOCE is also involved in vascular pathology. For example, SOCE mediates pulmonary vascular remodeling in patients with hypoxia-mediated pulmonary hypertension (42). Therefore, targeting SOCE may contribute to preventing VSMC proliferation in occlusive and proliferative disorders of the vessel wall.

As stated above, NSAIDs inhibit VSMC proliferation and DNA synthesis *in vivo* and *in vitro* without cellular toxicity and independently of cyclooxygenase (4, 6, 7). Consistently, our results show that NSAIDs diminish A10 cell proliferation at roughly the same concentrations that inhibit SOCE. The little disconnect between both parameters in some cases could be related to the facts that acute and chronic effects of NSAIDs could not be entirely similar and that a little component of A10 cell proliferation is independent of Ca^{2+} entry. The effects of NSAIDs cannot be explained by cell death, anti-inflammatory activity, or VOCE inhibition because cell viability was not decreased, structural analogs lacking anti-inflammatory activity (*(R)*-flurbiprofen) mimicked inhibition, and NSAIDs did not

prevent VOCE. Therefore, SOCE inhibition underlies the antiproliferative effects of NSAIDs in VSMCs.

NSAIDs may inhibit SOCE acting directly on channels or, alternatively, by targeting a regulatory mechanism. Our results favor this latter option for several reasons. First, NSAIDs do not inhibit CRAC directly. This conclusion is based in our studies with RBL cells. NSAIDs inhibit SOCE in RBL cells but do not prevent Icrac in strong Ca^{2+} buffer. However, in weak Ca^{2+} buffer, where mitochondrial Ca^{2+} uptake is essential for sustaining CRAC/Orai channels, NSAIDs significantly reduced Icrac. Second, SOCE (but not VOCE) promotes mitochondrial Ca^{2+} uptake in A10 cells. Third, SOCE (but not VOCE) is largely inhibited when mitochondrial Ca^{2+} uptake is impaired by mitochondrial depolarization with protonophores. These compounds are not selective to mitochondria, and they may collapse the proton gradient in any acidic organelle. As some of these acidic organelles have been reported to act as agonist-sensitive Ca^{2+} stores, protonophore effects should be regarded with caution. Finally, NSAIDs depolarize mitochondria and impair mitochondrial Ca^{2+} uptake in A10 cells, an action consistent with previous reports on the effects of salicylate and NSAIDs as mitochondrial uncouplers in both isolated mitochondria and intact cells (35, 41). Interestingly, NSAIDs added after VOCE produce the same effects than FCCP. It has been reported that mitochondria may regulate CRAC channels by production of ATP which supposedly acts as a calcium buffer (43). However, the finding that ruthenium red blocks CRAC confirms that mitochondrial Ca^{2+} buffering is an important factor. Moreover, ATP levels do not change upon exposure to NSAIDs.

Taken together, our results suggest that NSAIDs prevent mitochondrial Ca^{2+} uptake, thus facilitating the Ca^{2+} -dependent inactivation of SOC channels rather than inhibiting SOC channels directly. As SOCE is clearly involved in VSMC proliferation, this mechanism may underlie the antiproliferative and salutary effects of NSAIDs on proliferative disorders of the vascular wall.

REFERENCES

- Beech, D. J. (2007) *Biochem. Soc. Trans.* **35**, 890–894
- House, S. J., Potier, M., Bisailon, J., Singer, H. A., and Trebak, M. (2008) *Pflugers Arch.* **456**, 769–785
- Khan, Q., and Mehta, J. L. (2005) *J. Atheroscler. Thromb.* **12**, 185–190
- Marra, D. E., Simoncini, T., and Liao, J. K. (2000) *Circulation* **102**, 2124–2130
- Marra, D. E., and Liao, J. K. (2001) *Trends Cardiovasc. Med.* **11**, 339–344
- Brooks, G., Yu, X. M., Wang, Y., Crabbe, M. J., Shattock, M. J., and Harper J.V. (2003) *J. Pharm. Pharmacol.* **55**, 519–526
- Weber, A., Yildirim, H., and Schrör, K. (2000) *Eur. J. Pharmacol.* **389**, 67–69
- Anderson, H. V., McNatt, J., Clubb, F. J., Herman, M., Maffrand, J. P., DeClerck, F., Ahn, C., Buja, L. M., and Willerson, J. T. (2001) *Circulation* **104**, 2331–2337
- Gu, Q., Chen, J. L., and Ruan, Y. M. (2005) *Zhongguo Yi Xue Ke Xue Yuan Xue Bao* **27**, 87–91
- Guibert, C., Ducret, T., and Savineau, J. P. (2008) *Prog. Biophys. Mol. Biol.* **98**, 10–23
- Sonkusare, S., Palade, P. T., Marsh, J. D., Telemaque, S., Pesic, A., and Rusch, N. J. (2006) *Vascul. Pharmacol.* **44**, 131–142
- Parekh, A. B., and Putney, J. W., Jr. (2005) *Physiol. Rev.* **85**, 757–810
- Schwarz, E. C., Kummerow, C., Wenning, A. S., Wagner, K., Sappok, A., Waggesshauser, K., Griesemer, D., Strauss, B., Wolfs, M. J., Quintana, A., and Hoth, M. (2007) *Eur. J. Immunol.* **37**, 2723–2733
- Hoth, M., Fanger, C. M., and Lewis, R. S. (1997) *J. Cell Biol.* **137**, 633–648
- Hoth, M., Button, D. C., and Lewis, R. S. (2000) *Proc. Natl. Acad. Sci. U.S.A.* **97**, 10607–10612
- Gilabert, J. A., and Parekh, A. B. (2000) *EMBO J.* **19**, 6401–6407
- Glitsch, M. D., Bakowski, D., and Parekh, A. B. (2002) *EMBO J.* **21**, 6744–6754
- Quintana, A., Schwindling, C., Wenning, A. S., Becherer, U., Rettig, J., Schwarz, E. C., and Hoth, M. (2007) *Proc. Natl. Acad. Sci. U.S.A.* **104**, 14418–14423
- Liou, J., Kim, M. L., Heo, W. D., Jones, J. T., Myers, J. W., Ferrell, J. E., Jr., and Meyer, T. (2005) *Curr. Biol.* **15**, 1235–1241
- Feske, S., Gwack, Y., Prakriya, M., Srikanth, S., Puppel, S. H., Tanasa, B., Hogan, P. G., Lewis, R. S., Daly, M., and Rao, A. (2006) *Nature* **441**, 179–185
- Luik, R. M., Wang, B., Prakriya, M., Wu, M. M., and Lewis, R. S. (2008) *Nature* **454**, 538–542
- Li, J., Sukumar, P., Milligan, C. J., Kumar, B., Ma, Z. Y., Munsch, C. M., Jiang, L. H., Porter, K. E., and Beech, D. J. (2008) *Circ. Res.* **103**, e97–104
- Wang, Y., Deng, X., Hewavitharana, T., Soboloff, J., and Gill, D. L. (2008) *Clin. Exp. Pharmacol. Physiol.* **35**, 1127–1133
- Peel, S. E., Liu, B., and Hall, I. P. (2008) *Am. J. Respir. Cell Mol. Biol.* **38**, 744–749
- Takahashi, Y., Watanabe, H., Murakami, M., Ono, K., Munehisa, Y., Koyama, T., Nobori, K., Iijima, T., and Ito, H. (2007) *Biochem. Biophys. Res. Commun.* **361**, 934–940
- Ng, L. C., McCormack, M. D., Airey, J. A., Singer, C. A., Keller, P. S., Shen, X. M., and Hume, J. R. (2009) *J. Physiol.* **587**, 2429–2442
- Dietrich, A., Kalwa, H., Storch, U., Mederos y Schnitzler, M., Salanova, B., Pinkenburg, O., Dubrovskaya, G., Essin, K., Gollasch, M., Birnbaumer, L., and Gudermann, T. (2007) *Pflugers Arch.* **455**, 465–477
- DeHaven, W. I., Jones, B. F., Petranka, J. G., Smyth, J. T., Tomita, T., Bird, G. S., and Putney, J. W., Jr. (2009) *J. Physiol.* **587**, 2275–2298
- Potier, M., Gonzalez, J. C., Motiani, R. K., Abdullaev, I. F., Bisailon, J. M., Singer, H. A., and Trebak, M. (2009) *FASEB J.* **23**, 2425–2437
- Berra-Romani, R., Mazzocco-Spezia, A., Pulina, M. V., and Golovina, V. A. (2008) *Am. J. Physiol. Cell Physiol.* **295**, C779–790
- Aubart, F. C., Sassi, Y., Coulombe, A., Mougnot, N., Vrignaud, C., Lepince, P., Lechat, P., Lompré, A. M., and Hulot, J. S. (2009) *Mol. Ther.* **17**, 455–462
- Guo, R. W., Wang, H., Gao, P., Li, M. Q., Zeng, C. Y., Yu, Y., Chen, J. F., Song, M. B., Shi, Y. K., and Huang, L. (2009) *Cardiovasc. Res.* **81**, 660–668
- Hoth, M., and Penner, R. (1992) *Nature* **355**, 353–356
- Rao, R. S., Miano, J. M., Olson, E. N., and Seidel, C. L. (1997) *Cardiovasc. Res.* **36**, 118–126
- Núñez, L., Valero, R. A., Senovilla, L., Sanz-Blasco, S., García-Sancho, J., and Villalobos, C. (2006) *J. Physiol.* **571**, 57–73
- Valero, R. A., Senovilla, L., Núñez, L., and Villalobos, C. (2008) *Cell Calcium* **44**, 259–269
- Villalobos, C., Núñez, L., Montero, M., García, A. G., Alonso, M. T., Chamero, P., Alvarez, J., and García-Sancho, J. (2002) *FASEB J.* **16**, 343–353
- Villalobos, C., Alonso, M. T., and García-Sancho, J. (2009) *Methods Mol. Biol.* **574**, 203–214
- Zitt, C., Strauss, B., Schwarz, E. C., Spaeth, N., Rast, G., Hatzelmann, A., and Hoth, M. (2004) *J. Biol. Chem.* **279**, 12427–12437
- Ren, J., Albinsson, S., and Hellstrand, P. (2010) *J. Biol. Chem.* **285**, 31829–31839
- Gutknecht, J. (1990) *J. Membr. Biol.* **115**, 253–260
- Fantozzi, I., Zhang, S., Platoshyn, O., Remillard, C. V., Cowling, R. T., and Yuan, J. X. (2003) *Am. J. Physiol. Lung Cell. Mol. Physiol.* **285**, L1233–1245
- Montalvo, G. B., Artalejo, A. R., and Gilabert, J. A. (2006) *J. Biol. Chem.* **281**, 35616–35623